Letter

Dissipative quantum dynamics, phase transitions, and non-Hermitian random matrices

Mahaveer Prasad [1,*] Hari Kumar Yadalam [1,2,†] Camille Aron,[2,‡] and Manas Kulkarni[1,§]

[1] *International Centre for Theoretical Sciences, Tata Institute of Fundamental Research, 560089 Bangalore, India*

[2] *Laboratoire de Physique de l'École Normale Supérieure, ENS, Université PSL, CNRS, Sorbonne Université, Université Paris Cité, F-75005 Paris, France*

(Received 13 January 2022; accepted 26 April 2022; published 11 May 2022)

We explore the connections between dissipative quantum phase transitions and non-Hermitian random matrix theory. For this, we work in the framework of the dissipative Dicke model which is archetypal of symmetry-breaking phase transitions in open quantum systems. We establish that the Liouvillian describing the quantum dynamics exhibits distinct spectral features of integrable and chaotic character on the two sides of the critical point. We follow the distribution of the spacings of the complex Liouvillian eigenvalues across the critical point. In the normal and superradiant phases, the distributions are two-dimensional Poisson and that of the Ginibre unitary random matrix ensemble, respectively. Our results are corroborated by computing a recently introduced complex-plane generalization of the consecutive level-spacing ratio distribution. Our approach can be readily adapted for classifying the nature of quantum dynamics across dissipative critical points in other open quantum systems.

DOI: 10.1103/PhysRevA.105.L050201

Introduction. The notions of integrability and chaos are well formulated for classical interacting (nonlinear) systems [1–10]. Similar concepts for quantum mechanical systems have not reached the same level of maturity. Classically, integrable versus chaotic features are typically diagnosed by computing Lyapunov exponents [5,9,11–13] or by establishing the existence of an extensive number of independent conserved quantities (Liouville integrability) [7,14–18]. Attempts to generalize these diagnostics to the quantum realm have led, on the one hand, to the definition of Lyapunov exponents from the exponential growth of out-of-time-order correlators [19,20] and, on the other hand, to identifying sets of commuting operators. The presence, or lack thereof, of an extensive number of these operators manifests itself in the statistical features of the spectrum of the Hamiltonian [1,21–26].

The spectra of quantum Hamiltonians were conjectured to typically exhibit two distinct behaviors depending on whether their corresponding classical limits are integrable or chaotic. Initially, Berry, Tabor [27] speculated that typical quantum Hamiltonians with an integrable classical limit (except for a few pathological cases) have consecutive level spacings distributed according to the Poisson distribution. Later, Bohigas, Giannoni, and Schmit [28] further conjectured that those Hamiltonians with a chaotic classical limit have spectra exhibiting strong level repulsion and the consecutive level spacings are distributed according to Hermitian random matrix theory (RMT). Subsequent works have shown that these conjectures are also applicable to those quantum systems that do not have a well-defined classical limit [29–38].

These ideas were later extended to the case of Markovian open quantum systems. Instead of studying the spectrum of the isolated Hamiltonian H, i.e., the generator of closed quantum dynamics, one may study the spectrum of the Liouvillian $\mathcal{L}$, i.e., the generator of the evolution of the density matrix ρ, $\partial_t \rho = \mathcal{L}\rho$. Here, $\mathcal{L}$ accounts for both the unitary evolution and for the driven-dissipative processes induced by the coupling to the environment [39]. Generically, Liouvillians are non-Hermitian operators with complex spectra. Grobe, Haake, and Sommers [40] conjectured that those Liouvillians whose corresponding classical dynamics are integrable have complex level spacings distributed according to the two-dimensional (2D) Poisson distribution. On the contrary, those whose classical limits are chaotic follow the predictions from non-Hermitian RMT, specifically from the Ginibre ensembles [21,41,42]. More recently, these conjectures were also found to be valid for systems without a well-defined classical limit [43–45].

The simple intuition behind those successful conjectures goes as follows. For integrable dynamics with an extensive number of commuting conserved quantities, the spectrum of the Hamiltonian or the Liouvillian is expected to be the direct sum of extensively many independent sectors of the theory. This independence guarantees that levels within different sectors can overlap. On the other hand, for chaotic dynamics, only a few conserved quantities exist and level repulsion is expected in each symmetry sector. In turn, this presence or lack thereof of an extensive number of conserved quantities is expected to be reflected in the nearest-level spacing statistics of the spectra.

Studies on spectral properties of dissipative quantum evolutions have also focused on features of the eigenvalue density [46]. In particular, the Weyl law for isolated quantum systems [47] was generalized to open quantum systems [48–51].

In this work, we study the spectral properties of the Liouvillian of a dissipative version of the paradigmatic Dicke

*mahaveer.prasad@icts.res.in
†hari.kumar@icts.res.in
‡aron@ens.fr
§manas.kulkarni@icts.res.in

model [52,53]. In the thermodynamic limit, the isolated Dicke model displays a $\mathbb{Z}_2$-symmetry-breaking quantum phase transition between a normal and a superradiant phase [54–56]. Studies of the spectral statistics of the Dicke Hamiltonian [57,58] revealed that the level spacings are Poisson distributed in the normal phase, reflective of integrable dynamics, whereas they are distributed according to the Gaussian orthogonal ensemble in the superradiant phase, indicating chaotic dynamics. Here, via exact diagonalization of the Liouvillian, we discuss whether and how these connections with RMT can be generalized to the context of phase transitions in open quantum systems. More precisely, we address the robustness of the signatures of integrability as the system is driven through a phase transition by turning on an integrability-breaking perturbation.

Dissipative Dicke model. The dissipative Dicke model describes the coupling of an ensemble of closely packed quantum emitters to a single leaky cavity mode [52,53]. In the Markovian approximation, the evolution of the density matrix ρ is governed by a Lindblad master equation where the Liouvillian superoperator reads

$$\mathcal{L}\star = -i[H,\star] + \kappa[2a\star a^\dagger - \{a^\dagger a, \star\}], \tag{1}$$

where $\kappa > 0$ is the cavity decay rate and $\star$ stands for operators on the Hilbert space. The Dicke Hamiltonian is given by

$$H = \omega_c a^\dagger a + \omega_s S^z + \frac{2\lambda}{\sqrt{S}}(a^\dagger + a)S^x, \tag{2}$$

where a ($a^\dagger$) is the bosonic annihilation (creation) operator of a cavity mode with energy ω_c; S^α, $\alpha = x$, y, and z, are the spin angular momentum operators built from the totally symmetric representation of S identical two-level systems with energy splitting ω_s; and λ is the cavity-spin coupling which is rescaled by $1/\sqrt{S}$ to ensure a nontrivial thermodynamic limit ($S \to \infty$). The Dicke Hamiltonian is $\mathbb{Z}_2$ symmetric: $[H, \Pi] = 0$, where the operator $\Pi = \exp[i\pi(a^\dagger a + S^z + S/2)]$ gives the parity of the total number of excitations. As a consequence of the specific structure of the dissipator in Eq. (1), the Liouvillian inherits a so-called weak $\mathbb{Z}_2$ symmetry: $[\mathcal{L}, \mathit{\Pi}] = 0$, where $\mathit{\Pi}\star = \Pi \star \Pi^\dagger$ gives the parity of the difference of the number of excitations between the left and right sides of the states in Liouville space [59–61] (see also the Appendixes). In the thermodynamic limit, this weak $\mathbb{Z}_2$ symmetry is spontaneously broken in the steady state at $\lambda = \lambda^* = \frac{1}{2}\sqrt{\omega_c\omega_s}\sqrt{1+\kappa^2/\omega_c^2}$, corresponding to a second-order dissipative phase transition [56,62,63]. In the normal phase, i.e., $\lambda < \lambda^*$, the boson expectation value vanishes: $\langle a\rangle = 0$. In the superradiant phase, i.e., $\lambda > \lambda^*$, it acquires a finite expectation value: $\langle a\rangle \neq 0$. At $\lambda = 0$, the model is trivially integrable. The counterrotating terms, $a^\dagger S^+$ and aS^-, break the quantum integrability of the model.

Complex spectra. We analyze the statistical properties of the complex eigenvalues $\{E_i\}$ of the Liouvillian operator $\mathcal{L}$ by means of extensive numerical computations. We work in the even-parity sector of the Liouville space to avoid possible spurious overlaps of eigenvalues from the different symmetry sectors [64]. Throughout the paper, we consider the strongly dissipative regime, $\omega_c = \omega_s = \kappa = 1$, for which the critical point is located at $\lambda^* = 1/\sqrt{2} \approx 0.71$.

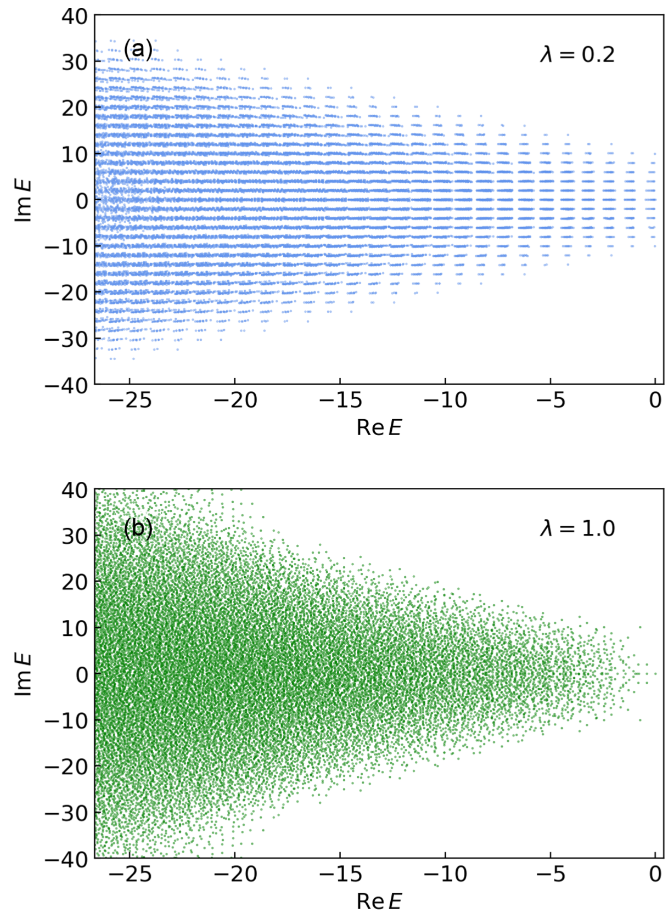

FIG. 1. Scatter plot of the complex spectrum of the Liouvillian $\mathcal{L}$ of the dissipative Dicke model for $S = 10$ and $\omega_c = \omega_s = \kappa = 1$ for which $\lambda^* = 1/\sqrt{2}$. (a) Normal phase, $\lambda = 0.2$. (b) Superradiant phase, $\lambda = 1.0$. A stark difference in the structure of the spectrum above and below the critical point can be observed.

In practice, the numerical approach comes with two inherent limitations.

(i) The infinitely large bosonic Hilbert space of the cavity has to be truncated to a finite number of excitations, $n_{\text{cutoff}} = 40$.

(ii) Numerical errors during the diagonalization process can propagate dangerously, yielding an accuracy of the results far worse than machine precision.

Consequently, we truncate our spectra to an energy window $\text{Re}\,E_i \in [-\alpha\kappa\, n_{\text{cuttoff}}, 0]$, where we make sure that statistics are converged with respect to n_{cutoff}. Although its precise value is of little consequence to our findings, we choose $\alpha = 2/3$. This amounts to analyzing the statistical properties of those eigenvalues which correspond to intermediate to long-lived dynamics. We work with 128-bit complex double float precision.

The overall aspect of the spectrum is illustrated in Fig. 1 for different values of the cavity-spin coupling λ and for fixed spin size $S = 10$. The symmetry about the real axis is a generic feature of Liouvillians of Lindblad master equations [24]. The unique steady-state of the dynamics corresponds to the single eigenvalue located at $E = 0$. The spectra in the two phases display clear differences. In the noninteracting limit, $\lambda = 0$, the spectrum displays ladder structures across both the imaginary and the real axis. The former are a direct consequence of our choice of resonant parameters, $\omega_c = \omega_s$, whereas the latter stem from the fragmentation of the Liouville space due to the presence of continuous symmetries at $\lambda = 0$: the weak U(1) symmetry corresponding to the conservation of superoperators $[a^\dagger a, \star]$ and the strong U(1) symmetry corresponding to the conservation of S^z. In the normal phase, $0 < \lambda < \lambda^*$, the spectrum in Fig. 1(a) still displays structured patterns that are inherited from the the noninteracting limit. The effect of a small but finite interaction can be seen as a renormalization of ω_c, ω_s, and κ, leading to smearing of the patterned spectrum. There, the existence of patterns across the real axis is robust and we suspect them to be rooted in the fragmentation of Liouville space due to the emergence of approximately conserved quantities. This fragmentation disappears as λ approaches λ^* and the spectrum does not display such signature of emergent conservation laws in the superradiant phase, $\lambda > \lambda^*$.

Spacing statistics of complex eigenvalues. In order to unveil the universal features of these complex spectra, we turn to the study of level-spacing statistics. We first perform an unfolding of the spectrum using standard procedures (see the Appendixes). The unfolded spectrum is then used to generate the histogram of the Euclidean distance s between nearest-neighbor eigenvalues in the complex plane, yielding the complex-level spacing distribution $p(s)$.

The results are summarized in Fig. 2 for values of λ corresponding to the normal and superradiant phases. For comparison, we also plot the corresponding spacing distribution for independent complex random numbers, namely, the 2D Poisson distribution,

$$p_{\text{2D-P}}(s) = \frac{\pi}{2} s \exp(-\pi s^2/4), \tag{3}$$

as well as the distribution for the eigenvalues of the corresponding non-Hermitian random matrix ensemble [40,44]. Given the absence of symmetry of our Liouvilian (the so-called *A* class), it corresponds to the Ginibre unitary ensemble (GinUE) [65–69],

$$p_{\text{GinUE}}(s) = \bar{s}\, \bar{p}_{\text{GinUE}}(\bar{s}s), \tag{4}$$

with

$$\bar{p}_{\text{GinUE}}(s) = \sum_{j=1}^{\infty} \frac{2s^{2j+1}\exp(-s^2)}{\Gamma(1+j, s^2)} \prod_{k=1}^{\infty} \frac{\Gamma(1+k, s^2)}{k!}, \tag{5}$$

and $\bar{s} = \int_0^\infty ds s \bar{p}_{\text{GinUE}}(s)$. Here, $\Gamma(1+k, s^2) = \int_{s^2}^\infty t^k e^{-t} dt$ is the incomplete Gamma function.

Figure 2 demonstrates that the distributions computed from the spectrum of $\mathcal{L}$ in Eq. (1) are in remarkable agreement with the 2D Poisson distribution in the normal phase and with the GinUE prediction in the superradiant phase. In the superradiant phase, this reflects the presence of complex-eigenvalue repulsion characterized by a $p(s) \sim s^3$ suppression at small energy spacings, which is consistent with Eq. (4). On the other hand, in the normal phase we find $p(s) \sim s$, consistent with Eq. (3). This corresponds to the absence of level repulsion in the 2D complex plane [24].

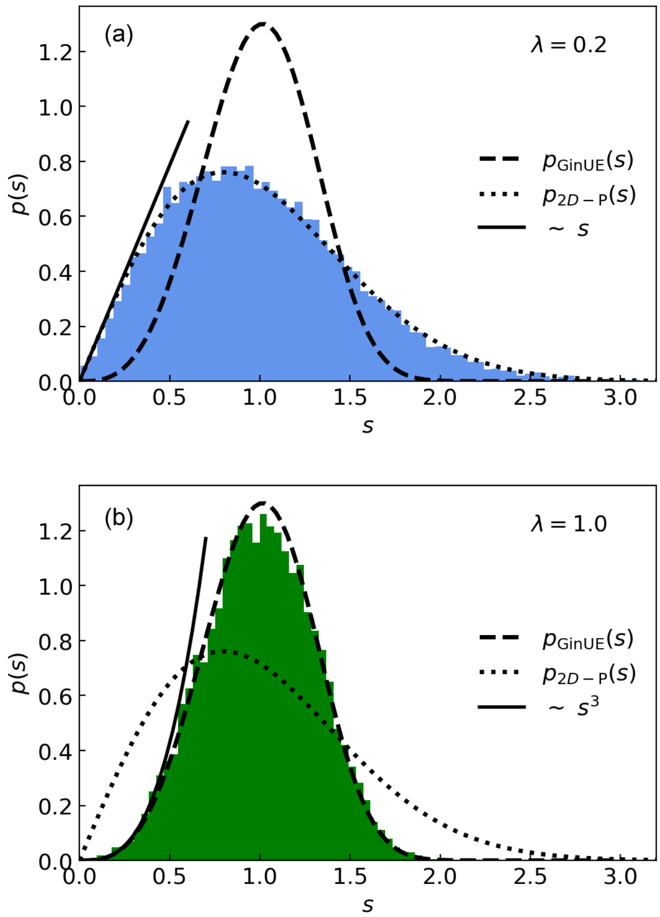

FIG. 2. Level-spacing distribution of the complex spectrum of the Liouvillian $\mathcal{L}$ in (a) the normal phase with $\lambda = 0.2$ and (b) the superradiant phase with $\lambda = 1.0$. We find remarkable agreement with the 2D Poisson distribution $p_{\text{2D-P}}(s)$ given in Eq. (3) and that of the GinUE RMT prediction $p_{\text{GinUE}}(s)$ given in Eq. (4) in the normal phase and in the superradiant phase, respectively.

In order to better quantify the nature of the statistics as one crosses from one phase to another, we introduce the metric motivated by Refs. [58,70,71]

$$\eta \equiv \frac{\int_0^\infty ds[p(s) - p_{\text{2D-P}}(s)]^2}{\int_0^\infty ds[p_{\text{GinUE}}(s) - p_{\text{2D-P}}(s)]^2}. \tag{6}$$

By construction, η vanishes when the numerically obtained distribution $p(s)$ approaches the 2D Poisson distribution, whereas η goes to 1 when $p(s)$ approaches the GinUE prediction. Figure 3, showing η versus λ, exhibits the crossover from a 2D Poisson distribution to that of GinUE prediction as one crosses the critical point. This crossover sharpens with increasing the system size.

Complex-plane generalization of the consecutive level-spacing ratio. Until now, we only probed spectral statistics using the Euclidean distance s between complex levels. In order to extract the angular information we resort to a recently introduced diagnostic [72] involving the level-spacing ratio,

$$z_i = r_i e^{i\theta_i} = \frac{E_i^{\text{NN}} - E_i}{E_i^{\text{NNN}} - E_i}, \tag{7}$$

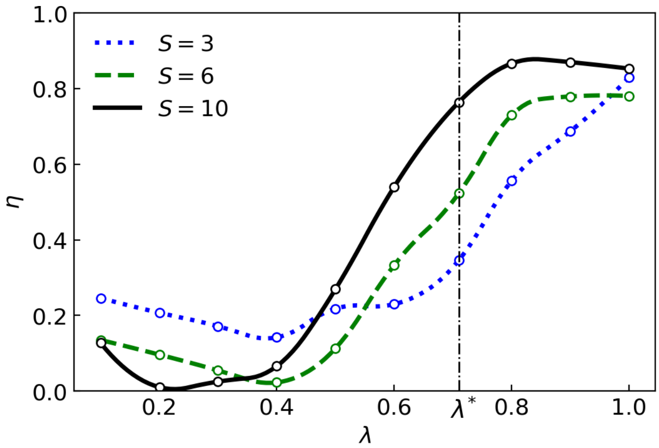

FIG. 3. The metric η defined in Eq. (6) as we increase the coupling λ from the normal phase to the superradiant phase. It shows the crossover of the complex-eigenvalue spacing distribution from integrable ($\eta \sim 0$) to RMT ($\eta \sim 1$) predictions. The crossover sharpens as we increase the system size. At $\lambda = 0$ the dissipative cavity decouples from the spin. Hence, the spectrum is expected to display pathological statistics away from any universal behavior. This explains the observed discrepancies close to $\lambda = 0$.

where superscripts NN (NNN) stand for nearest (next-nearest) neighbor. Equation (7) is the generalization of the well-known adjacent gap ratio [73,74] defined for isolated quantum systems. It captures information about next-nearest neighbors which is missed in the conventional diagnostics of level-spacing statistics. An additional advantage of this quantity is that it does not rely on the unfolding procedure which may sometimes be ambiguous and unreliable. In Fig. 4, we show the scatter plots of z_i below and above the critical point. The anisotropy in the superradiant phase is another signature of connection to RMT [72]. To quantitatively compare with the predictions of 2D Poisson distribution and GinUE RMT, we report $\langle r \rangle$ and $\langle \cos\theta \rangle$ for a range of λ values in the table below Fig. 4.

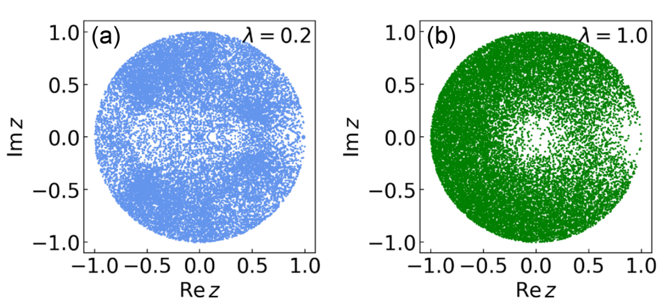

λ	2D Poisson	0.2	0.4	0.6	0.8	1.0	GinUE
-$\langle \cos\theta \rangle$	0	0.00	0.09	0.19	0.23	0.24	0.24
$\langle r \rangle$	0.67	0.69	0.71	0.72	0.74	0.74	0.74

FIG. 4. Scatter plot of the complex level-spacing ratio z introduced in Eq. (7) for $S = 10$ (a) in the normal phase, $\lambda = 0.2$, and (b) in the superradiant phase, $\lambda = 1.0$. The table gives $\langle \cos\theta \rangle$ and $\langle r \rangle$ for a range of λ values, along with their prediction from the 2D Poisson distribution and GinUE RMT.

Conclusion. We investigated how the presence of a dissipative quantum phase transition driven by an integrability-breaking term affects the spectral statistics of the complex Liouvillian spectrum of open quantum systems. Working in the framework of the dissipative Dicke model, we found the spectral features of integrability to be robust against the integrability-breaking perturbation until the onset of the dissipative quantum phase transition. In the symmetry-broken phase, they are eventually replaced by RMT features indicative of chaotic dynamics. While our results unambiguously reveal a tight connection between dissipative quantum phase transition driven by the integrability-breaking term and spectral phase transition of the Liouvillian, whether they happen simultaneously at $\lambda = \lambda^*$ has yet to be scrutinized. The approach we developed here can be straightforwardly adapted to other dissipative quantum dynamics. This will be instrumental to further establish whether this robustness of integrability features against integrability-breaking terms is a general trait in the context of open quantum systems.

H.K.Y., C.A., and M.K. are grateful for the support from Project No. 6004-1 of the Indo-French Centre for the Promotion of Advanced Research (IFCPAR). M.K. acknowledges the support of a Ramanujan Fellowship (Grant No. SB/S2/RJN-114/2016), a SERB Early Career Research Award (Grant No. ECR/2018/002085), and a SERB Matrics Grant (Grant No. MTR/2019/001101) from the Science and Engineering Research Board (SERB), Department of Science and Technology, Government of India. M.K. acknowledges support from the Department of Atomic Energy, Government of India, under Project No. RTI4001. C.A. acknowledges the support from the French ANR "MoMA" under Project No. ANR-19-CE30-0020. M.K. thanks the hospitality of the École Normale Supérieure (Paris).

APPENDIX A: COMPUTING THE SPECTRUM OF THE DISSIPATIVE DICKE LIOUVILLIAN

We use a convenient basis of the Liouville space spanned by the states

$$|\alpha\rangle\rangle \equiv ||n_l, m_l\rangle\langle n_r, m_r|\,\rangle, \tag{A1}$$

where $|n, m\rangle$ are the Fock states of the Dicke Hamiltonian with n cavity excitations and $m = -S/2, -S/2 + 1, \dots, S/2$ is the quantum number associated with the z component of the spin. α collects all the quantum numbers n_l, m_l, n_r, and m_r. The notation $|\alpha\rangle\rangle$ underlines that operators on the Hilbert space are states in the Liouville space. In practice, we truncate the Hilbert and Liouville spaces by introducing a cavity cutoff: $n = 0, 1, \dots, n_{\rm cutoff}$. In the above basis, the Liouvillian can be represented by a matrix L with the elements $L_{\alpha\alpha'} = \langle\langle \alpha|\mathcal{L}|\alpha'\rangle\rangle$, where the Hilbert-Schmidt inner product [24,75] is given by

$$\langle\langle \alpha|\alpha'\rangle\rangle \equiv {\rm Tr}[(|n_l, m_l\rangle\langle n_r, m_r|)^\dagger |n_l', m_l'\rangle\langle n_r', m_r'|] \tag{A2}$$

and the trace is performed over the Hilbert space. Let us recall that $\mathcal{L}$ has a parity symmetry [59–61], $[\mathcal{L}, \varPi] = 0$, where the superoperator $\varPi$ acts on the basis states as

$$\varPi|\alpha\rangle\rangle = \varPi|n_l, m_l\rangle\langle n_r, m_r| = \zeta\,|\alpha\rangle\rangle, \tag{A3}$$

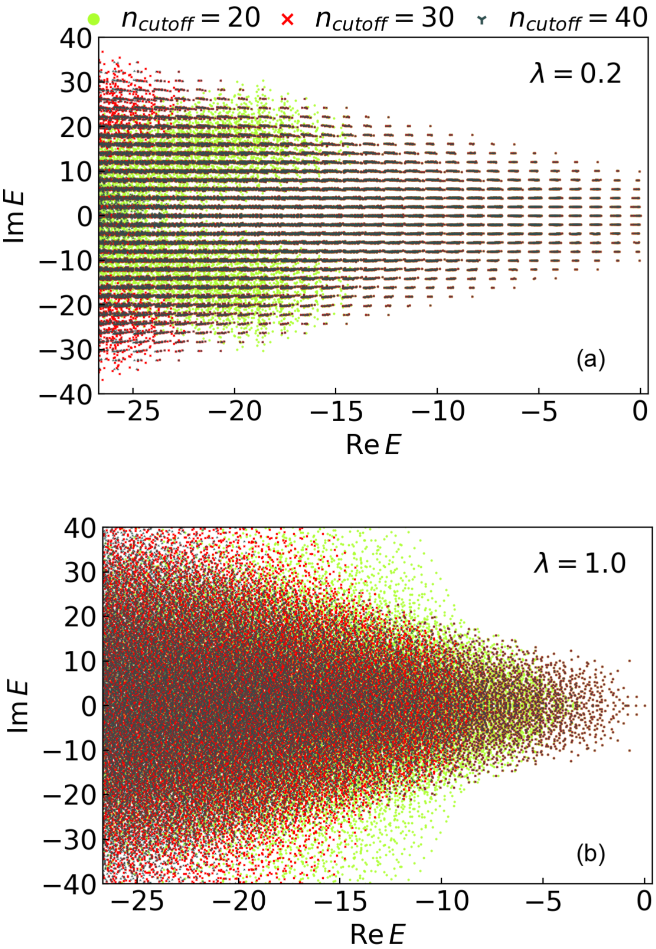

FIG. 5. Scatter plot of the Liouvillian spectrum of the dissipative Dicke model for different $n_{\text{cutoff}} = 20$, 30, and 40 in (a) the normal phase, $\lambda = 0.2$, and (b) the superradiant phase, $\lambda = 1.0$ ($S = 10$).

with $\zeta = +1$ if $(n_l + m_l) - (n_r + m_r)$ is even and $\zeta = -1$ if it is odd. This weak $\mathbb{Z}_2$ symmetry of $\mathcal{L}$ guarantees that it does not couple states of the Liouville space with different parities. Hence, L can be organized as a two-by-two block-diagonal matrix. To avoid spurious overlaps of eigenvalues, we discard the odd-parity block. Finally, the even-parity block matrix is fed to a diagonalization algorithm of the LAPACK library suited to complex non-Hermitian matrices.

APPENDIX B: UNFOLDING THE COMPLEX SPECTRUM

To eliminate the system-specific features of the level-spacing statistics, we first perform an unfolding procedure of the spectrum. Several methods have been proposed for the case of a complex spectrum [66,76]. We use the method of Ref. [44]. First, we compute the Euclidean distance of each of the N complex eigenvalues to its nearest neighbor (NN)

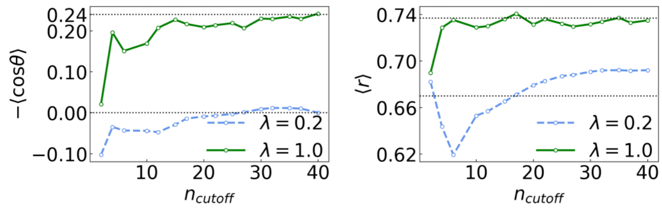

FIG. 6. $\langle\cos\theta\rangle$ and $\langle r\rangle$ versus n_{cutoff}, computed from the consecutive complex level-spacing ratio distribution of z introduced in Eq. (7) ($S = 10$).

$s_i \equiv |E_i - E_i^{\text{NN}}|$. Next, we rescale these distances as

$$s_i \to s_i' = s_i \frac{\sqrt{\rho_{\text{av}}(E_i)}}{\bar{s}}, \tag{B1}$$

where $\rho_{\text{av}}(E_i)$ is the local average density approximated by

$$\rho_{\text{av}}(E) = \frac{1}{2\pi\sigma^2 N}\sum_{i=1}^{N}\exp\left(-\frac{|E - E_i|^2}{2\sigma^2}\right) \tag{B2}$$

and σ is chosen greater than the global mean level spacing given by $\tilde{s} = (1/N)\sum_{i=1}^{N} s_i$. This guarantees a smooth distribution function on the scale of $\tilde{s}$. In practice, we work with $\sigma = 4.5 \times \tilde{s}$. $\bar{s}$ in Eq. (B1) is set to ensure that the global mean level spacing of the s_i' is unity: $(1/N)\sum_{i=1}^{N} s_i' = 1$. Finally, the statistics of nearest-level spacings are computed from the s_i'. In the main text, we drop the prime notation in s_i' for the sake of simplicity.

APPENDIX C: CONVERGENCE OF THE STATISTICAL PROPERTIES OF THE SPECTRUM WITH RESPECT TO THE CAVITY CUTOFF

While the introduction of a finite n_{cutoff} is essential to the numerical diagonalization of the Liouvillian, the repercussions on the resulting spectrum must be dealt with care. In Fig. 5, we plot the spectrum of $\mathcal{L}$ both in the normal and in the superradiant phase for different values of $n_{\text{cutoff}} = 20$, 30, and 40 and focusing on the window $\text{Re}E \in [-\frac{2}{3} \times 40\,\kappa, 0]$. In the normal phase, the three cutoffs yield the same highly patterned spectrum in the window $\text{Re}E \in [-10\,\kappa, 0]$. The patterned region of the spectrum grows as n_{cutoff} is increased. For $n_{\text{cutoff}} = 40$, the whole window $\text{Re}E \in [-\frac{2}{3} \times 40\,\kappa, 0]$ is patterned. In the superradiant phase, convergence is obtained in the window $\text{Re}E \in [-5\,\kappa, 0]$. Rather than convergence of the eigenvalues, it is more important to ensure the convergence of their spectral statistics. In Fig. 6, we follow the convergence of properties extracted from the consecutive level-spacing ratio distribution [72] introduced in Eq. (7). Both $\langle r\rangle$ and $\langle\cos\theta\rangle$ remarkably converge when $n_{\text{cutoff}} \approx 30$. All results presented in the main text were produced with $n_{\text{cutoff}} = 40$.

[1] L. E. Reichl, *The Transition to Chaos* (Springer, Berlin, 1992).

[2] S. H. Strogatz, *Nonlinear Dynamics and Chaos* (Westview, Boulder, CO, 1996).

[3] H. Goldstein, C. Poole, and J. Safko, *Classical Mechanics* (Addison-Wesley, Boston, 2002).

[4] V. I. Arnol'd, *Mathematical Methods of Classical Mechanics*, Graduate Texts in Mathematics Vol. 60 (Springer, Berlin, 2013).

[5] M. Lakshmanan and S. Rajaseekar, *Nonlinear Dynamics: Integrability, Chaos and Patterns* (Springer, Berlino, 2012).

[6] J. Thompson and H. Stewart, *Nonlinear Dynamics and Chaos* (Wiley, New York, 2002).
[7] G. M. Zaslavsky, *Hamiltonian Chaos and Fractional Dynamics* (Oxford University, Oxford, 2004).
[8] K. Alligood, T. Sauer, and J. Yorke, *Chaos: An Introduction to Dynamical Systems*, Textbooks in Mathematical Sciences (Springer, Berlin, 2000).
[9] T. Tél, M. Gruiz, K. Kulacsy, and S. Hadobas, *Chaotic Dynamics: An Introduction Based on Classical Mechanics*, (Cambridge University, Cambridge, England, 2006).
[10] P. Cvitanović, R. Artuso, R. Mainieri, G. Tanner, and G. Vattay, *Chaos: Classical and Quantum* (Niels Bohr Inst., Copenhagen, 2016).
[11] A. M. Lyapunov, Int. J. Control **55**, 531 (1992).
[12] J. P. Eckmann and D. Ruelle, Rev. Mod. Phys. **57**, 617 (1985).
[13] L. Arnold and V. Wihstutz, *Lyapunov Exponents*, Lecture Notes in Mathematics (Springer-Verlag, Berlin, Heidelberg, 1986).
[14] M. A. Olshanetsky and A. M. Perelomov, Classical integrable finite-dimensional systems related to Lie algebras, Phys. Rep. **71**, 313 (1981).
[15] A. Das, *Integrable Models*, Lecture Notes in Physics Vol. 30 (World Scientific, Singapore, 1989).
[16] O. Babelon, D. Bernard, and M. Talon, *Introduction to Classical Integrable Systems* (Cambridge University, Cambridge, England, 2003).
[17] G. Arutyunov, *Elements of Classical and Quantum Integrable Systems* (Springer, Berlin, 2019).
[18] G. Sardanashvily, *Handbook of Integrable Hamiltonian Systems* (URRS, Moscow, 2015).
[19] A. Larkin and Y. N. Ovchinnikov, Sov. Phys. JETP **28**, 1200 (1969).
[20] J. Maldacena, S. H. Shenker, and D. Stanford, J. High Energy Phys. 08 (2016) 106.
[21] M. L. Mehta, *Random Matrices* (Elsevier, Amsterdam, 2004).
[22] G. Akemann, J. Baik, and P. Di Francesco, *The Oxford Handbook of Random Matrix Theory* (Oxford University, Oxford, 2011).
[23] T. Guhr, A. Müller-Groeling, and H. A. Weidenmüller, Phys. Rep. **299**, 189 (1998).
[24] F. Haake, in *Quantum Coherence in Mesoscopic Systems* (Springer, Berlin, 1991), pp. 583–595.
[25] H.-J. Stöckmann, *Quantum Chaos: An Introduction* (Cambridge University, Cambridge, England, 1999).
[26] M. C. Gutzwiller, *Chaos in Classical and Quantum Mechanics*, Interdisciplinary Applied Mathematics Vol. 1 (Springer, Berlin, 2013).
[27] M. V. Berry and M. Tabor, Proc. R. Soc. London, Ser. A **356**, 375 (1977).
[28] O. Bohigas, M. J. Giannoni, and C. Schmit, Phys. Rev. Lett. **52**, 1 (1984).
[29] T. A. Brody, J. Flores, J. B. French, P. A. Mello, A. Pandey, and S. S. M. Wong, Rev. Mod. Phys. **53**, 385 (1981).
[30] T. C. Hsu and J. C. Anglès d'Auriac, Phys. Rev. B **47**, 14291 (1993).
[31] V. Zelevinsky, B. Brown, N. Frazier, and M. Horoi, Phys. Rep. **276**, 85 (1996).
[32] V. Kota, Phys. Rep. **347**, 223 (2001).
[33] L. F. Santos, J. Phys. A **37**, 4723 (2004).
[34] K. Kudo and T. Deguchi, J. Phys. Soc. Jpn. **74**, 1992 (2005).
[35] L. F. Santos and M. Rigol, Phys. Rev. E **81**, 036206 (2010).
[36] A. Pal and D. A. Huse, Phys. Rev. B **82**, 174411 (2010).
[37] A. Gubin and L. F. Santos, Am. J. Phys. **80**, 246 (2012).
[38] D. A. Abanin, E. Altman, I. Bloch, and M. Serbyn, Rev. Mod. Phys. **91**, 021001 (2019).
[39] H.-P. Breuer and F. Petruccione, *The Theory of Open Quantum Systems* (Oxford University, Oxford, 2002).
[40] R. Grobe, F. Haake, and H.-J. Sommers, Phys. Rev. Lett. **61**, 1899 (1988).
[41] J. Ginibre, J. Math. Phys. (NY) **6**, 440 (1965).
[42] P. J. Forrester, *Log-Gases and Random Matrices* (Princeton University, Princeton, NJ, 2010).
[43] R. Hamazaki, K. Kawabata, and M. Ueda, Phys. Rev. Lett. **123**, 090603 (2019).
[44] G. Akemann, M. Kieburg, A. Mielke, and T. Prosen, Phys. Rev. Lett. **123**, 254101 (2019).
[45] Y. Huang and B. I. Shklovskii, Phys. Rev. B **101**, 014204 (2020).
[46] F. Borgonovi, I. Guarneri, and D. L. Shepelyansky, Phys. Rev. A **43**, 4517 (1991).
[47] H. P. Baltes, *Spectra of Finite Systems: A Review of Weyl's Problem, the Eigenvalue Distribution of the Wave Equation for Finite Domains and its Applications on the Physics of Small Systems* (Bibliographisches Institut, Mannheim, 1976).
[48] W. T. Lu, S. Sridhar, and M. Zworski, Phys. Rev. Lett. **91**, 154101 (2003).
[49] D. L. Shepelyansky, Phys. Rev. E **77**, 015202(R) (2008).
[50] S. Nonnenmacher and M. Rubin, Nonlinearity **20**, 1387 (2007).
[51] L. Ermann and D. L. Shepelyansky, Eur. Phys. J. B **75**, 299 (2010).
[52] R. H. Dicke, Phys. Rev. **93**, 99 (1954).
[53] M. Gross and S. Haroche, Phys. Rep. **93**, 301 (1982).
[54] B. M. Garraway, Philos. Trans. R. Soc. London, Ser. A **369**, 1137 (2011).
[55] K. Hepp and E. H. Lieb, Ann. Phys. (NY) **76**, 360 (1973).
[56] P. Kirton, M. M. Roses, J. Keeling, and E. G. Dalla Torre, Adv. Quantum Technol. **2**, 1800043 (2019).
[57] C. Emary and T. Brandes, Phys. Rev. Lett. **90**, 044101 (2003).
[58] C. Emary and T. Brandes, Phys. Rev. E **67**, 066203 (2003).
[59] V. V. Albert and L. Jiang, Phys. Rev. A **89**, 022118 (2014).
[60] B. Buča and T. Prosen, New J. Phys. **14**, 073007 (2012).
[61] S. Lieu, R. Belyansky, J. T. Young, R. Lundgren, V. V. Albert, and A. V. Gorshkov, Phys. Rev. Lett. **125**, 240405 (2020).
[62] F. Dimer, B. Estienne, A. S. Parkins, and H. J. Carmichael, Phys. Rev. A **75**, 013804 (2007).
[63] M. M. Roses and E. G. Dalla Torre, PLoS ONE **15**, e0235197 (2020).
[64] N. Rosenzweig and C. E. Porter, Phys. Rev. **120**, 1698 (1960).
[65] D. Bernard and A. LeClair, in *Statistical Field Theories* (Springer, Berlin, 2002), p. 207.
[66] R. Hamazaki, K. Kawabata, N. Kura, and M. Ueda, Phys. Rev. Research **2**, 023286 (2020).
[67] T. Kanazawa and T. Wettig, Phys. Rev. D **104**, 014509 (2021).
[68] A. M. García-García, L. Sá, and J. J. Verbaarschot, arXiv:2110.03444.
[69] We are assuming that the positivity-conservation property of Liouvillians is irrelevant to spacing distribution of the Ginibre unitary ensemble [24].

[70] B. I. Shklovskii, B. Shapiro, B. R. Sears, P. Lambrianides, and H. B. Shore, Phys. Rev. B **47**, 11487 (1993).
[71] B. Georgeot and D. L. Shepelyansky, Phys. Rev. Lett. **81**, 5129 (1998).
[72] L. Sá, P. Ribeiro, and T. Prosen, Phys. Rev. X **10**, 021019 (2020).
[73] V. Oganesyan and D. A. Huse, Phys. Rev. B **75**, 155111 (2007).
[74] Y. Y. Atas, E. Bogomolny, O. Giraud, and G. Roux, Phys. Rev. Lett. **110**, 084101 (2013).
[75] S. Mukamel, *Principles of Nonlinear Optical Spectroscopy*, Oxford Series in Optical and Imaging Sciences Vol. 6 (Oxford University, Oxford, 1999).
[76] H. Markum, R. Pullirsch, and T. Wettig, Phys. Rev. Lett. **83**, 484 (1999).